

MECHANICAL AND MICROSTRUCTURAL PROPERTIES
OF DUPLEX STEELMIKROSTRUKTURA IN MEHANSKE LASTNOSTI DUPELKS
JEKELMIRKO GOJIĆ¹, L. KOSEC², L. VEHOVAR³¹Željezara Sisak, Sektor za razvoj, B. Adžije 2, 44000 Sisak, Croatia²OMM, Naravoslovnotehniška fakulteta, Ljubljana³Inštitut za kovinske materiale in tehnologijo, Ljubljana*Prejem rokopisa - received: 1997-05-26; sprejem za objavo - accepted for publication: 1997-10-21*

In this work mechanical properties and microstructure of duplex steel after heat treatment are shown. Heat treatment of the steel consisted of water quenching from 1050°C. A ferrite-austenite microstructure was obtained and the brittle σ -phase was avoided. The results show that the impact energy depends on the direction of rolling. In rolling direction the share of ferrite and austenite was approximately equal.

Key words: duplex steel, mechanical properties, ferrite-austenite microstructure, impact energy

V članku so opisani rezultati raziskav mikrostrukture in mehanskih lastnosti dupleks jekel po gašenju v vodi s 1050°C. Na ta način je jeklo dobilo mikrostrukturo iz ferita in austenita in brez krhke σ -faze. Rezultati kažejo, da je udarna energija odvisna od smeri valjanja. Na vzdolžnem prerezu cevi sta deleža ferita in austenita približno enaka.

Ključne besede: dupleks jeklo, mehanske lastnosti, feritno-austenitna mikrostruktura, udarna energija

1 INTRODUCTION

Because of excellent strength and toughness as well as high resistance to corrosion the high alloy stainless steels are used in car, electronic and petrochemical industries. Investigations of the development of high alloy steels which have simultaneously a high strength and other physical-chemical characteristics are important¹. Depending on chemical composition, especially the content of chromium, nickel, and carbon as well as heat treatment high alloy steels can have a ferrite, austenite, martensite or duplex microstructure. Between the high alloy steels duplex stainless steel (DSS) with austenite-ferrite microstructure has an important role²⁻⁶. It is a relatively new class of engineering material for different applications because of the excellent combination of mechanical and corrosion characteristics. DSS offer benefits over austenite stainless steels and carbon steels because of their higher strength, good toughness and ductility in combination with equivalent resistance to general corrosion, as well as better resistance to localized corrosion and stress corrosion cracking. Today DSS have low carbon content (<0.002 wt.%) and contain optimal contents of chromium, nickel, molybdenum, copper and nitrogen for obtaining the required properties.

In process industries materials with a favorable microstructure are used because it determines their mechanical and corrosion behavior. DSS with a austenite-ferrite microstructure are desirable, if free of brittle σ -phase⁷. In the present work the investigation of mechanical and microstructural properties of DSS after heat

treatment are presented with the accent on impact energy and the share of phases.

2 EXPERIMENTAL

2.1 Material

A section of commercially produced duplex stainless tubing was used for this investigation. The thermal treatment consisted of solution annealing at 1050°C and water quenching. The chemical composition the steel is given in **Table 1**.

Table 1: Chemical composition of duplex stainless steel, wt. %

C	Si	Mn	P	S	Cr	Mo	Al	Ni	N
0.02	0.45	0.88	0.024	0.018	24.97	3.19	0.04	8.20	0.12

2.2 Mechanical and microstructural testing

The mechanical properties were assessed on an Instron 1196 tensile testing machine in accordance with standard ASTM procedures⁸. The average hardness was determined by the Brinell method (HB), while the microhardness of austenite and ferrite grains was determined using the indenter on a Leitz-Wetzlar optical microscope 8196. Impact testing was performed at room temperature in both directions of rolling.

Microstructural tests were carried out with optical microscopy (OM), scanning electron microscopy (SEM), transmission electron microscopy (TEM), image analysis system and X-rays diffraction (XRD). Specimens for metallographic analysis were mechanically polished and

Table 2: Results of mechanical properties of duplex steel

R_e MPa	R_m MPa	A %	Z %	Hardness HB	Microhardness HV _{0.10}	Impact energy J
645	774	33	53	225	$\alpha = 140$ $\gamma = 292$	dir. of rolling: 41 transverse to dir. of rolling: 33

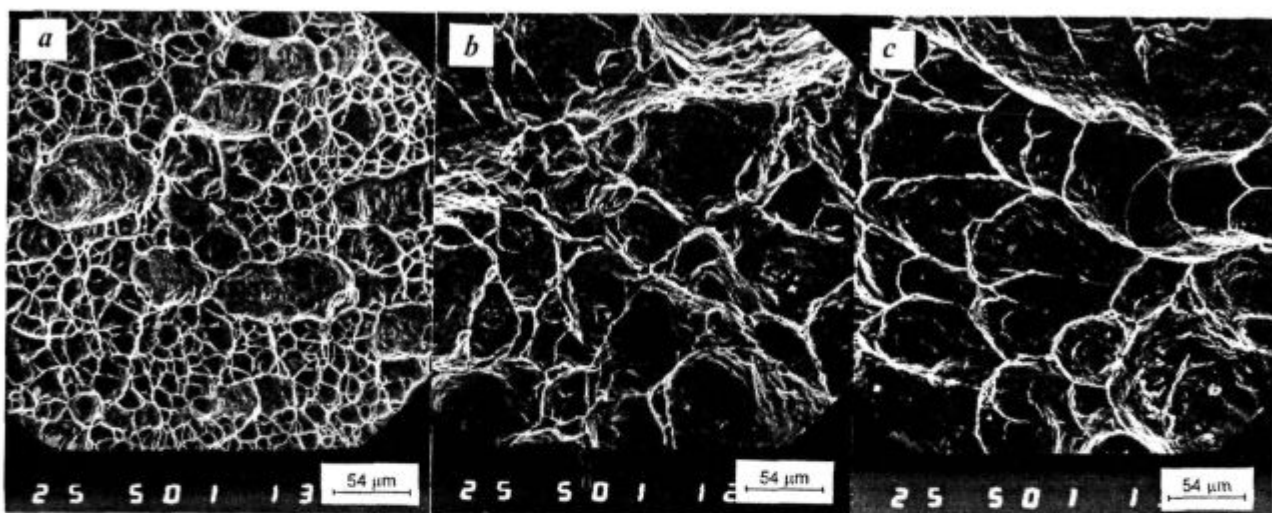


Figure 1: Microfractography of fracture surface of duplex steel after tensile testing (a) and impact testing in longitudinal (b) and transverse direction (c)

Slika 1: Mikrofraktografije prelomnih površin dupleksa jekla po raztržnem preiskusu (a) in preiskusu udarne žilavosti v vzdolžni (b) in v prečni smeri valjanja (c)

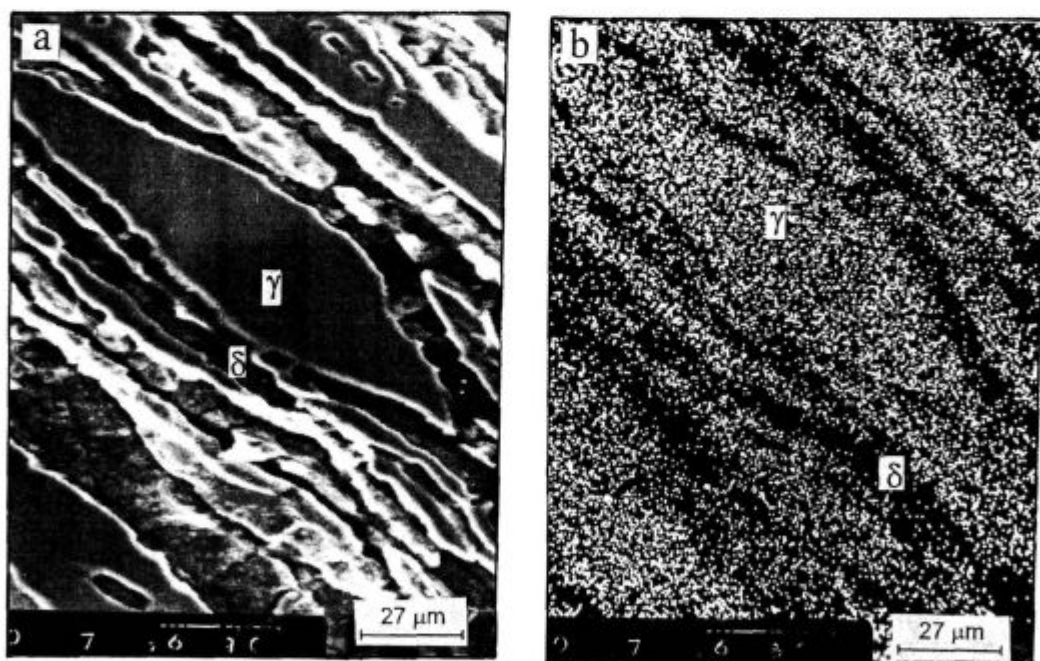


Figure 2: Scanning electron microscopy image of duplex steel in longitudinal direction (a) and the scanning picture for nickel (b)

Slika 2: Raster elektronski posnetek dupleksa jekla v vzdolžni smeri valjanja (a) in x slika niklja (b)

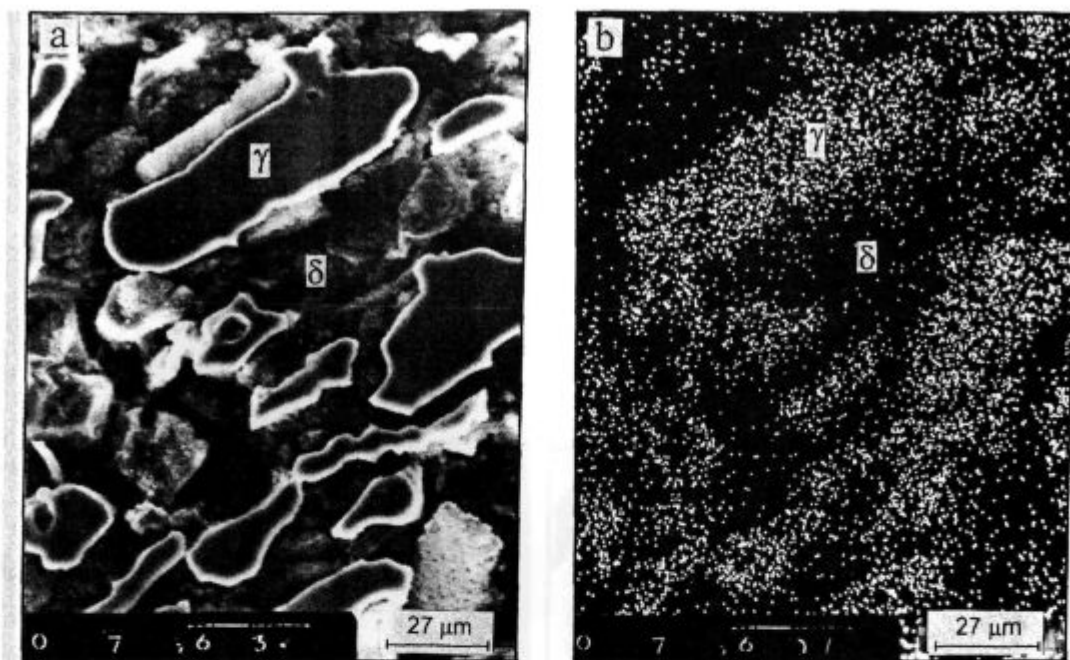


Figure 3: Scanning electron microscopy image of duplex steel in transverse direction (a) and the scanning picture for nickel (b)
 Slika 3: Raster elektronski posnetek dupleks jekla prečno na smer valjanja (a) in x slika niklja (b)



Figure 4: Optical (a) and transmission electron bright-field micrographs (b) of duplex steel. D - twins
 Slika 4: Optični (a) in transmissijski elektronski posnetek (b) dupleks jekla. D - dvojčki

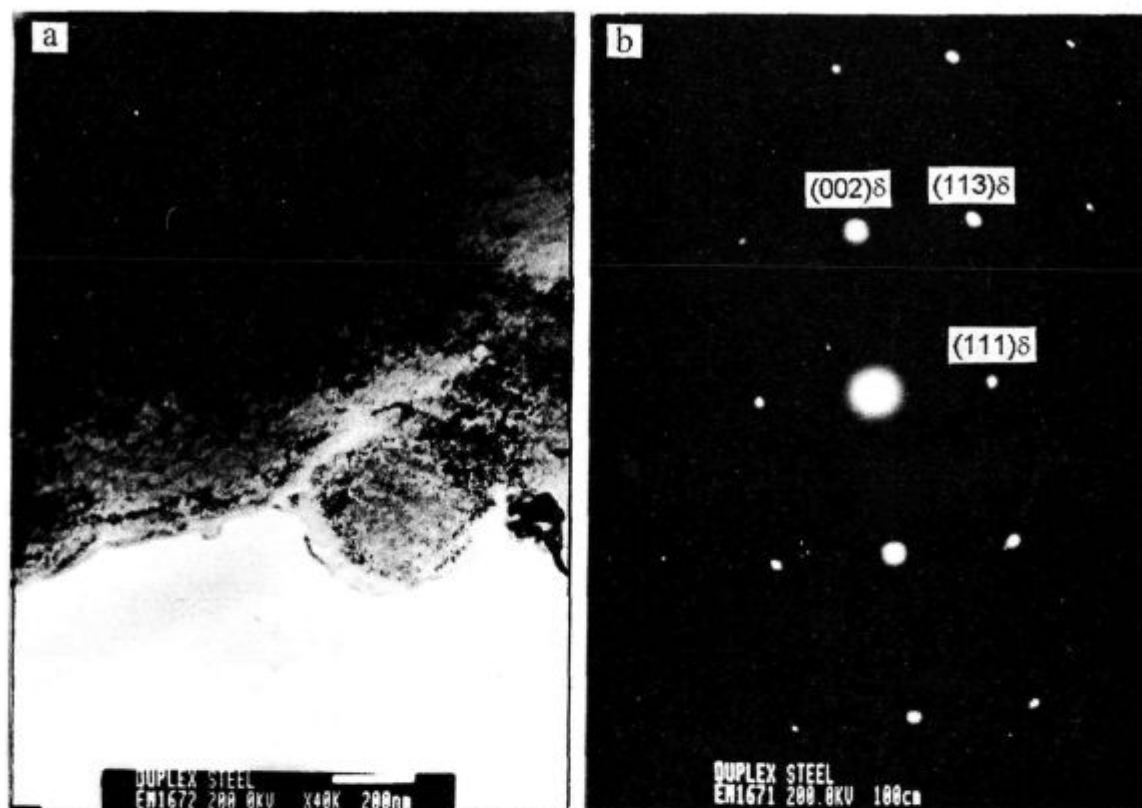


Figure 5: Transmission electron microscopy bright-field micrograph of ferrite phase (a) with indexed area diffraction pattern (b)
Slika 5: Transmisijski elektronski posnetek feritne faze (a) z indeksirano difrakcijo za ferit (b)

etched in the Kallings reagent, an acid chloride solution (1.5 g of CuCl_2 , 33 ml of HCl, 33 ml alcohol and 33 ml of distilled water)⁹. The microstructure was examined in optical and SE microscopes, which was equipped for wave dispersive X-ray (WDX) analysis. The quantitative shares of ferrite and austenite were determined using an image analysis system. Thin foil samples for transmission electron microscope were prepared electrochemically and examined TEM operated at 200 kV and equipped for diffraction analysis. The phase identification was obtained by X-rays diffraction using $\text{CuK}\alpha$ radiation.

3 RESULTS

Mechanical properties (R_e - yield strength, R_m - tensile strength, A - elongation and Z - reduction of area), impact energy, hardness and microhardness of DSS were measured at room temperature on three specimens. The average values of the properties are given in Table 2. When compared to usual stainless steels DSS have a significantly higher yield strength (twice that of austenite steels) and a good impact energy. However, the steel showed also a significant anisotropy in impact energy. The fracture process and valuable evidence concerning the cause of failure can be obtained through microfrac-

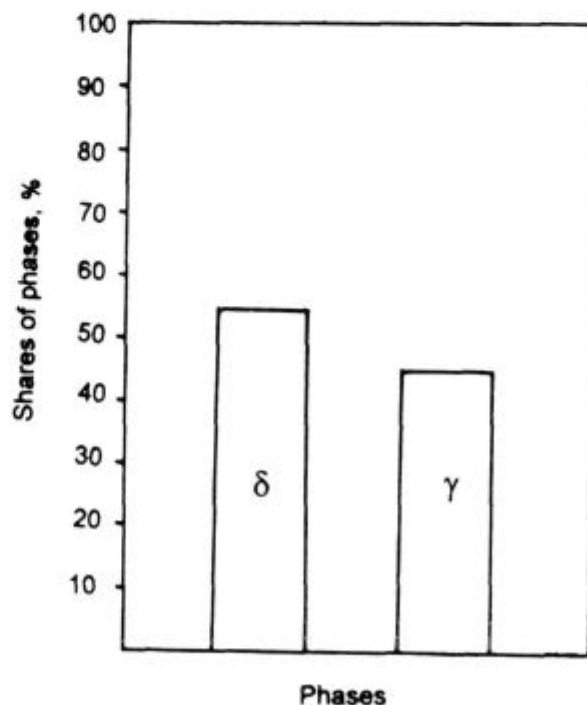


Figure 6: Quantitative shares of the ferrite-austenite microstructure in rolling direction
Slika 6: Kvantitativni delež ferita in austenita v mikrostrukturi v vzdolžni smeri valjanja

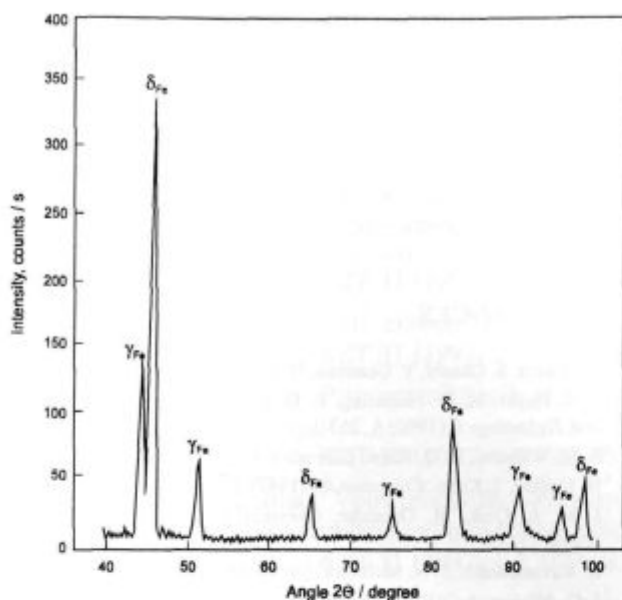


Figure 7: X-ray diffraction spectrum of duplex stainless steel
Slika 7: X-ray difrakcijski spekter dupleks jekel

tography¹⁰. **Figure 1** shows the fracture surfaces of DSS after tensile and impact testing. The difference in fracture surfaces is only in size of dimples. At tensile testing DSS fracture in the ductile mode by microvoid coalescence mechanism (**Figure 1a**). The fracture surfaces after impact testing are also ductile but with elongated dimples (**Figures 1b and 1c**).

Figures 2 and 3 show the microstructure of DSS in both rolling directions. In both directions the microstructure is similar and consists of austenite grains embedded

in ferrite. In rolling direction austenite grains are more elongated. Austenite grains contain more and ferrite grains less nickel (**Figures 2b and 3b**). No σ -phase was found also by TEM observation, while frequent twins were observed in ferrite grains (arrow D, **Figure 4a**), which was identified by selected area diffraction (SAD) pattern (**Figure 5**). **Figure 6** shows the results of the quantitative phase analysis in rolling direction. An average of the ten continuous fields was used for estimation of the phase share. In the longitudinal direction the shares of ferrite and austenite were approximately equal. **Figure 7** shows the X-ray spectrum of the steel. The phases were identified using of JCPDS data¹¹. Only the presence of ferrite and austenite was confirmed by X rays diffraction.

4 DISCUSSION

The microstructure and the depending mechanical and corrosion properties are explained the best through the solidification process according to the quasi binary FeCrNi phase diagram, which is shown schematically in **Figure 8**¹² with dashed lines locating the DSS. By equilibrium solidification, δ -ferrite is the primary solidification phase. δ -ferrite then undergoes solid-state transformation in a two-phase region consisting of austenite (γ) and ferrite (δ) as the temperature is lowered. The nucleation of austenite occurs at grain boundaries enriched in carbon and nitrogen because of their limited solubility in ferrite. Given sufficient time, soluble carbon and nitrogen in solid solution diffuse uniformly throughout the austenite phase. It is known that a slow cooling under 815°C or aging at about 850°C can result in the formation of σ -phase¹³, which is prevented by a final solution annealing at 1050°C and water quenching, as shown already. In this case a microstructure consisting of approximately equal shares of austenite and ferrite in the rolling direction is obtained. Taking into account the chromium and nickel equivalents¹⁴ the properties of both phases (δ and γ) and their respective compositions can be approximately calculated for a given alloy and annealing temperature. The DSS tested here was represented in **Figure 8** by the dashed lines. It can be seen that at 1050°C for the composition given in **Table 1**, the steel is located in the two phases $\delta+\gamma$ region having an approximate δ/γ fraction of 55:45 in accordance to the share of phases shown in **Figure 6** for the rolling direction.

The high tensile strength (**Table 2**) is the result of several simultaneous mechanisms¹⁵: interstitial solid solution hardening (carbon and nitrogen); substitutional solid solution hardening (chromium, molybdenum and nickel) and strengthening by grain refinement (the presence of two phases prevents their mutual growth during heat treatment). The values of impact energy are higher in the longitudinal than in the transverse direction of rolling. Thus, the properties of DSS depend on the shape and arrangement of both phases as well as on the direc-

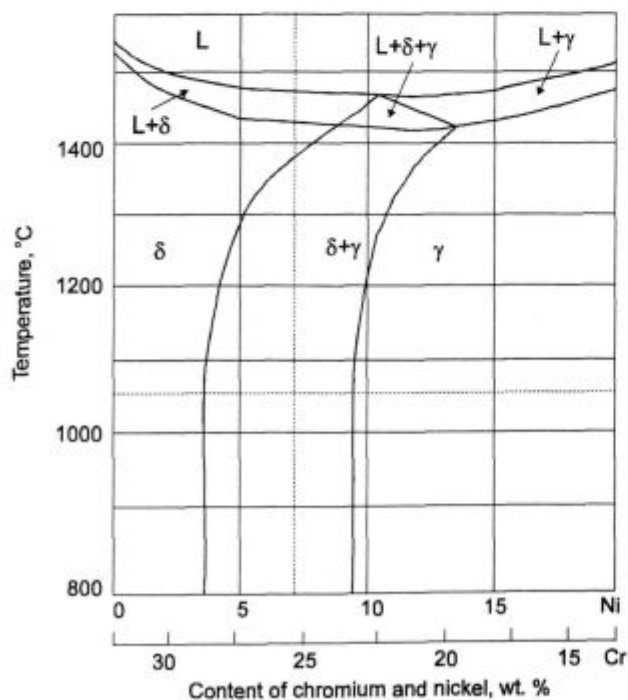


Figure 8: Quasi binary diagram of FeCrNi alloy with located duplex steel

Slika 8: Kvazi binarni diagram Fe-Cr-Ni z lokacijo dupleks jekel

tion of rolling. The difference in micromorphology fracture is explained through the fracture stresses and shape of both phases. The effect of deformation mode is usually explained in terms of localized shear deformation¹⁶. Probably, also the interface between the austenite and ferrite in DSS plays a considerable role in the fracture process. Crack propagation may take place through austenite and ferrite grains. The propagation is associated with the interface it depends greatly on the orientation of ferrite and austenite stringers¹⁷. There is a tendency of the propagation cracks to deflect along the interface to produce delamination when stringers lie parallel to the applied stress.

Taking into consideration the microstructural texture (Figure 2a), as well as their microhardness lower impact energy in transverse to the direction was expected. A higher ductility of DSS in the longitudinal direction of rolling could indicate to the crack propagation along the δ/γ boundaries because of axial stress, in contrast to the transverse direction of rolling where the fracture is produced by orthogonal stresses. This is in agreement with the results by Odelstam¹⁸ showing that elongation is by DSS lower in the transverse than in longitudinal direction.

5 CONCLUSION

In this work the results of investigation of mechanical and microstructural properties of the duplex stainless steel (DSS) are shown the heat treating consisted of annealing at 1050°C and water quenching, which produced a ferrite-austenite microstructure free of brittle σ -phase. Compared with usual stainless steels the DSS has a significantly higher mechanical strength (twice higher yield strength than that of austenite steels) with a good impact energy. It was found that the impact energy depends on

the direction of rolling. In the longitudinal direction of rolling the fractions of the ferrite and austenite were approximately equal. A higher ductility of steel in rolling direction could indicate to the crack propagation along the boundaries because of axial stress, in contrast to the transverse direction of rolling where the fracture produced by orthogonal stress.

6 REFERENCES

- ¹ Y. Murata, S. Ohashi, Y. Uematsu, *ISIJ International* 33 (1993) 7, 711
- ² F. H. Hayes, M. G. Hathering, R. D. Longbottom, *Materials Science and Technology* 6 (1990) 6, 263
- ³ S. M. Wilhelm, R. D. Kane, *Corrosion* 40 (1984) 8, 431
- ⁴ N. Sridhar, J. Kolts, *Corrosion* 43 (1987) 11, 646
- ⁵ J. M. A. Quik, M. Geudeke, *Chemical Engineering Progress* 11 (1994) 11, 49
- ⁶ K. Ravindranath, S. N. Malhotra, *Corrosion Science* 37 (1995) 2, 121
- ⁷ J. O. Nilsson, A. Wilson, *Materials Science and Technology* 9 (1993) 7, 545
- ⁸ ASTM standard E 370
- ⁹ *Metals Handbook* vol.8, Metals Park, OH: ASM, 1973, p. 99
- ¹⁰ Y. Tomita, *Materials Science and Technology* 11 (1995) 7, 508
- ¹¹ Search Manual for Selected Powder Diffraction Data for Metals and Alloys, JCPDS International Centre for Diffraction Data (eds. S. Weissmann), Pennsylvania, Swarthmore, 1978
- ¹² C. J. Long and W. T. DeLong, *Welding Journal* 62 (1983) 4, 281
- ¹³ Y. Maehara and Y. Ohmory, *The Sumitomo Search* 31 (1985) 11, 147
- ¹⁴ L. Pryce and K. W. Andrews, *Journal Iron Steel Institute* 196 (1969) 6, 415
- ¹⁵ J. Charles, M. Verneau and B. Bonnefois, *Proceedings 12th International Corrosion Congress*, Houston, Vol. 4, 1993, p. 2926
- ¹⁶ A. ul-Haq, H. Weiland and H. J. Bunge, *Materials Science and Technology* 10 (1994) 4, 289
- ¹⁷ T. P. Perng and C. J. Altstetter, *Metallurgical Transactions* 18A (1987) 2, 123
- ¹⁸ T. Odelstam, *Proc. Conf. Pulp and Paper Industry Corrosion*, Stockholm Vol. 4, 1983, p. 140